An analysis of the role of active site protic residues of cytochrome *P*-450s: mechanistic and mutational studies on 17α-hydroxylase-17,20-lyase (*P*-450$_{17\alpha}$ also CYP17)

Peter LEE-ROBICHAUD, Monika E. AKHTAR and Muhammad AKHTAR[1]

Department of Biochemistry, University of Southampton, Bassett Crescent East, Southampton SO16 7PX, U.K.

Certain cytochrome *P*-450s involved in the transformation of steroids catalyse not only the hydroxylation process associated with the group of enzymes, but also an acyl-carbon cleavage reaction. The hydroxylation occurs using an iron-monooxygen species while the acyl-carbon cleavage has been suggested to be promoted by an iron peroxide. In this paper we have studied the role of active site protic residues, Glu^{305} and Thr^{306}, in modulating the two activities. For this purpose, the kinetic parameters for the hydroxylation reaction (pregnenolone → 17α-hydroxypregnenolone) and two different versions of acyl-carbon cleavage (17α-hydroxypregnenolone → dehydro*epi*androsterone and 3β-hydroxyandrost-5-ene-17β-carbaldehyde → 3β-hydroxyandrost-5,16-diene + androst-5-ene-3β,17α-diol) were determined using the wild-type human CYP17 and its eight different single and double mutants. In addition the propensity of the proteins to undergo a subtle rearrangement converting the 450 nm active-form into an inactive counterpart absorbing at 420 nm, was monitored by measuring the $t_{\frac{1}{2}}$ of the *P*-450 → *P*-420 conversion. The results are interpreted to draw the following conclusions. The functional groups of Glu^{305} and Thr^{306} do not directly participate in the two proton delivery steps required for hydroxylation but may be important participants for the provision of a net work of hydrogen bonds for 'activating' water that then acts as a proton donor. The loss of any one of these residues is, therefore, only partially debilitating. That the mutation of Thr^{306} impairs the hydroxylation reaction more than it does the acyl-carbon cleavage is consistent with the detailed mechanistic scheme considered in this paper. Furthermore attention is drawn to the fact that the mutation of Glu^{305} and Thr^{306} subtly perturbed the architecture of the active site, which affects the geometry of this region of the protein and therefore its catalytic properties.

INTRODUCTION

A group of cytochromes *P*-450 to which CYP17 (17α-hydroxylase-17,20-lyase) belongs, catalyse not the only the conventional hydroxylation reaction but also an acyl-carbon bond cleavage (Scheme 1), that proceeds according to the stoichiometry of eqn. (1):

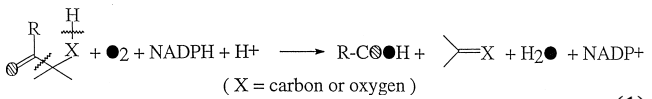

(1)

Our extensive studies on this class of enzymes [1–6] have led to the proposal that the two generic reactions are promoted by different species, acyl-carbon cleavage by an iron-peroxide intermediate (Fe^{III}–O–O^{-}) and hydroxylation by an oxo derivative (Fe^{IV}–$O^{\bullet}$). The suggestion was originally made to rationalize the results of $^{18}O_2$ experiments performed on CYP19 (aromatase) [1,2,7] and has received subsequent support from studies on certain liver *P*-450s [8–10], CYP17 [3,11], CYP51 [12,13] (sterol 14α-demethylase), NO synthase [14] and also biomimetic experiments [15]. The proposal has now been further scrutinized by site-directed mutagenesis of residues 305 to 309 of human CYP17, which from the known three-dimensional structures of soluble *P*-450s [16–18], may be deduced to be present at the active site region of the enzyme. To study the properties of the CYP17 mutants we exploited the distinctive feature of the enzyme that allows it to use three substrates, directing each towards a unique reaction course: hydroxylation (**1** → **2**) [19] and two specific versions of the acyl-carbon cleavages [11,19] (**2** → **3** and **4** → **5** + **6**).

EXPERIMENTAL

Materials

17α-Hydroxy[21-^{3}H]pregnenolone was prepared as described previously [20] and [17α-^{3}H]pregnenolone from 17α-bromopregnenolone [21], following debromination with Zn in $CH_3COO^{3}H$. Ni^{2+}-NTA-agarose and DNA purification kits were obtained from Qiagen Inc. Chatsworth (U.S.A.); endonucleases from Promega (U.K.), Chilworth Research Centre, Southampton; VENT$_R$ DNA polymerase from New England BioLabs (U.K.) Ltd., Hitchin, Hertfordshire; hydroxyapatite Bio Gel HTP from Bio-Rad Laboratories Ltd., Watford (U.K.). DNA primers were synthesized by Oswel DNA Service, University of Southampton (U.K.). All other chemicals were obtained from Sigma Chemical Co. (U.K.). The plasmid pCWH17mod, containing the modified human CYP17 gene, was a generous gift from Prof. Waterman, Vanderbilt University, Nashville, TN.

Polymerase chain reaction (PCR) mutagenesis

A plasmid (pCWH17mod) [22] in which the human CYP17 gene was modified at its 5′ end to allow its expression in *E. coli* and at its 3′ end with codons for four histidine residues was used in the

[1] To whom correspondence should be addressed.

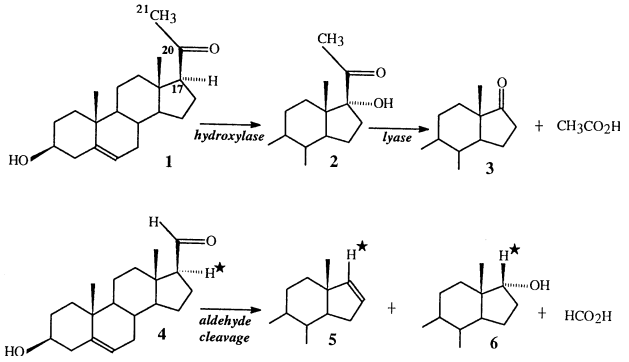

Scheme 1 The three reactions catalysed by CYP17

The conversions **2** → **3** and **4** → **5** + **6** represent different versions of acyl-carbon cleavage as further detailed by the lower sequence of Scheme 2. For the conversion **4** → **5** + **6** the status of the C-17 hydrogen atom of **4** is shown.

present work. At 1051 bp *Xba*I–*Sac*I fragment, encoding human CYP17 amino acids 102–452, was cut out of pCWH17mod and ligated into *Xba*I/*Sac*I double-digested pBluescript SK(−) (Stratagene, San Deigo, CA, U.S.A.). Synthetic oligonucleotides 5′-AACAGCTATGACCATG-3′ (**A**) and 3′-TGACCGGCAGC-AAAATG-5′ (**B**), corresponded to flanking sequences on each side of the inserted fragment. Mutagenesis was achieved in two PCR stages [23]. The first involved two separate PCR amplifications, one using the outside primer, **A**, with a primer of the series **C** (see legend to Table 1) and the other primer, **B**, together with a primer of the series **D** (Table 1). Each of the two reactions was performed in a final volume of 40 μl, containing outside and inside primer (300 ng each), template DNA (80 ng), 440 μM each dTNP, 4.5 mM $MgSO_4$, 10 mM KCl, 10 mM $(NH_4)_2SO_4$, 0.1% Triton X-100 and 20 mM Tris/HCl (pH 8.8, at 25 °C). The solutions were brought to 95 °C for 5 min, 1 unit of $VENT_R$ DNA polymerase was added and the temperature cycled between 94 °C (1 min), 55 °C (40 s) and 72 °C (45 s) for 30 cycles. The two PCR products, approx. 500 and 750 bp, were purified on agarose gel and combined in equal molar ratios (50:75 ng respectively) and functioned as template DNA for the final PCR, which was performed using only the two outside primers, **A** and **B**; all other components were as described above. After the addition of the $VENT_R$ DNA polymerase the temperature was cycled between 94 °C (1 min), 48 °C (1 min 10 s), 65 °C (1 min) for 5 cycles and 94 °C (1 min), 50 °C (45 s) and 72 °C (45 s) for 30 cycles. The PCR product was purified on agarose gel, digested with *Xba*I and *Sac*I and subcloned into pCWH17mod. Following the selection of the mutant clones, always the entire *Xba*I–*Sac*I fragment was sequenced to determine the position of the mutation and confirm that the remaining DNA was unaltered.

Expression and purification of proteins

Human CYP17 was expressed in *E. coli* and purified to a specific content of 10 nmol *P*-450/mg of protein as described previously [11]. This specific content compares favourably with other reported values for the human 10.7 [22] and the pig 8.0 [19] enzymes. Using the same method, the various mutant human CYP17 proteins were purified to between 85 and 95% homogeneity, and had specific contents ranging between 2.5 and 9.5 nmol *P*-450/mg of protein. These values are lower than the theoretical value of 18 because of variable loss of the non-covalently bound haem during the extreme environmental changes that occur during purification and partial conversion of *P*-450 to the inactive *P*-420 species. Porcine NADPH-cytochrome *P*-450 reductase [specific activity 35.5 units/mg of protein; 1 unit defined as 1 μmol of cytochrome *c* reduced per minute, at 35 °C, in potassium phosphate buffer (375 mM), pH 7.7] and porcine cytochrome b_5 (specific content 43.4 nmol haem/mg of protein) were purified as described in the literature [24,25].

Enzyme assays

Radio-labelled substrate (as detailed below), CYP17 (100 pmol), NADPH-cytochrome *P*-450 reductase (4.5 units), L-α-phosphatidylcholine dilauroyl (80 μg) and, when present, cytochrome b_5 (400 pmol) were mixed, reconstituted and the assay was performed as described under 'Incubation details' in a previous study [26]. The 0.03% sodium cholate carried with the stock of CYP17, necessary to prevent aggregation of this hydrophobic protein, was diluted to 0.00015% in the final assay volume of 1 ml. The release of $[^3H]H_2O$ from [17α-^{3}H]pregnenolone (**1**, specific activity 6.3×10^3 d.p.m./nmol; 75 nmol), $[^3H]CH_3COOH$ from [21-^{3}H]17α-hydroxypregnenolone (**2**, specific activity 4.4×10^4 d.p.m./nmol; 30 nmol) and [^{3}H]HCOOH from [20-^{3}H]3β-hydroxyandrost-5-ene-17β-carbaldehyde (**4**, specific activity 1.0×10^5 d.p.m./nmol; 80 nmol) was used for the quantification of the hydroxylase, lyase and aldehyde cleavage activity respectively, with aliquots removed for measuring at 0, 4, 8 and 12 min, 0, 2, 4 and 6 min and 0, 1, 2, 3 and 4 min respectively, as

Table 1 DNA primers used to generate the various CYP17 mutant proteins

Each primer shown represents the sense mutant primer and is of the series **D**, series **C** comprises the antisense primers that have a complementary sequence to those displayed in the table. The active site glutamate and threonine residues are in bold face and the base changes are highlighted by bold face lowercase.

Amino acid change	Primer sequence
Wild-type	(300) Phe- Gly- Ala- Gly- Val- **Glu**- **Thr**- Thr- Thr- Ser- Val (310)
	5′-C TTT GGG GCT GGC GTG GAG ACC ACC ACC TCT GTG G-3′
Glu^{305} → Gln	5′-C TTT GGG GCT GGC GTG **c**AG ACC ACC ACC TC-3′
Thr^{306} → Ala	5′-C TTT GGG GCT GGC GTG GAG **g**C**a** ACC ACC TC-3′
Thr^{307} → Ala	5′-C TTT GGG GCT GGC GTG GAG ACC **g**C**a** ACC TC-3′
Thr^{308} → Ala	5′-GGG GCT GGC GTG GAG ACC ACC **g**C**a** TCT GTG G-3′
Ser^{309} → Ala	5′-GGG GCT GGC GTG GAG ACC ACC ACC **g**CT GTG G-3′
Glu^{305} → Ala: **Thr**^{306} → Ala	5′-C TTT GGG GCT GGC GTG **c**AG **g**C**a** ACC ACC TC-3′
Glu^{305} → Ala: Thr^{308} → Ala	5′-GGG GCT GGC GTG **c**AG ACC ACC **g**C**a** TCT GTG G-3′
Glu^{305} → Ala: Ser^{309} → Ala	5′-GGG GCT GGC GTG **c**AG ACC ACC ACC **g**CT GTG G-3′

Table 2 Wild-type and mutant CYP17 hydroxylase (1 → 2), lyase (2 → 3) and aldehyde cleavage (4 → 5 + 6) activities

Experiments were performed in triplicate with the data expressed as means ± S.E. The glutamate and threonine active site residues are in bold face. N.D., Not determined (see text). Aldehyde cleavage : hydroxylase ratios for mutants having the Thr^{306} → Ala change are double underlined.

		Activity (nmol/min per nmol P450)						
CYP17 variant	b_5	Hydroxylase (**a**)	%	Lyase	%	Aldehyde (**4**) cleavage (**b**)	%	(**b**)/(**a**)
Wild-type	−	2.17 ± 0.04		0.32 ± 0.05		11.60 ± 1.14	100	
	+	3.30 ± 0.20	100	3.06 ± 0.05	100	N.D.		3.5
Glu^{305} → Gln	−	0.80 ± 0.07		< 0.05		5.73 ± 0.20	49	
	+	1.17 ± 0.06	35	0.65 ± 0.06	21	N.D.		4.9
Thr^{306} → Ala	−	0.15 ± 0.02		0.14 ± 0.01		4.86 ± 0.95	42	
	+	0.19 ± 0.02	6	0.89 ± 0.06	29	N.D.		<u>25.6</u>
Thr^{307} → Ala	−	0.80 ± 0.03		0.13 ± 0.01		4.70 ± 0.12	41	
	+	1.12 ± 0.02	34	1.00 ± 0.05	33	N.D.		4.2
Thr^{308} → Ala	−	2.17 ± 0.10		0.38 ± 0.01		12.15 ± 0.15	105	
	+	3.37 ± 0.13	102	3.85 ± 0.10	125	N.D.		3.6
Ser^{309} → Ala	−	1.48 ± 0.05		0.32 ± 0.02		7.11 ± 0.26	61	
	+	2.40 ± 0.10	73	2.70 ± 0.10	88	N.D.		3.0
Glu^{305} → Ala : **Thr^{306}** → Ala	−	< 0.02		< 0.02		0.97 ± 0.07	8	
	+	< 0.02	< 0.1	< 0.02	< 0.1	N.D.		<u>> 48.5</u>
Glu^{305} → Ala : Thr^{308} → Ala	−	1.07 ± 0.07		< 0.05		10.2 ± 0.10	88	
	+	1.47 ± 0.07	45	0.60 ± 0.12	20	N.D.		6.9
Glu^{305} → Ala : Ser^{309} → Ala	−	0.57 ± 0.08		< 0.02		7.90 ± 0.30	68	
	+	0.85 ± 0.06	26	0.50 ± 0.02	16	N.D.		9.3

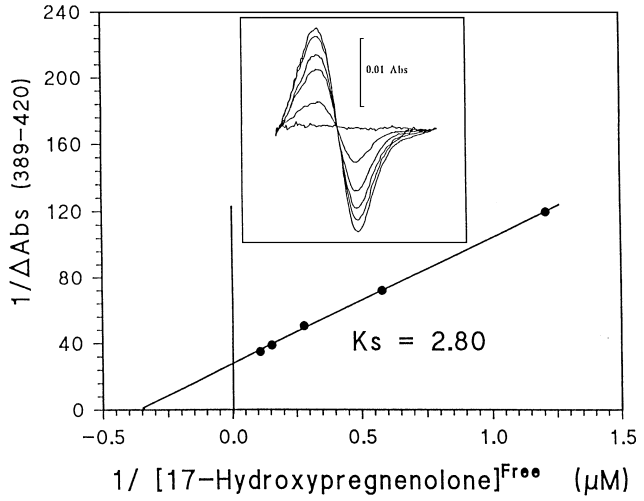

Figure 1 A typical 17α-hydroxypregnenolone-binding spectrum for the CYP17 mutant, Ser^{309} → Ala and its analysis to derive the dissociation constant

described for the ^3H release assay reported previously [26]. It should be noted that lyase activity shown with the wild-type CYP17 in Table 2 is almost twice that reported previously [11,26] because of the use of higher NADPH-cytochrome P450 reductase : CYP17 ratios in the present work. Another point to note is that because of the limited solubilities of **2**, the concentration of this substrate (30 μM) in the assay mixture is only approx. 3-fold higher than its K_s value with some of the mutants. In these cases the rates in Table 2 are estimated to be 75–80 % of the putative V_{max} values.

Measurement of K_s values

Pregnenolone- and 17α-hydroxypregnenolone-binding spectra were recorded on a Kontron Uvikon 930 spectrophotometer. Measurements were recorded over a period of 1 h which made it necessary to reduce the temperature to 12 °C due to the propensity of some mutants to undergo P450 → P420 conversion at higher temperatures (see next section and Results). A solution of purified CYP17 (1 μM), in potassium phosphate buffer [50 mM, pH 7.25, glycerol (20 % v/v) and sodium cholate (0.15 % w/v)] was placed in the sample and reference cuvette and a baseline recorded. Ligand (pregnenolone or 17α-hydroxypregnenolone, 1 mM in ethanol) was then added sequentially to give final concentrations in the cuvette of 1, 2, 4, 7 and 10 μM and the spectra recorded 10 min after each addition (see inset, Figure 1). K_s values were found from the reciprocal plot of $1/\Delta A_{389\text{-}420}$ against $1/[L]^{free}$ (Figure 1), having first calculated $[L]^{free}$ by linear extrapolation of the plot of $\Delta A_{389\text{-}420}$ against $\Delta A_{389\text{-}420}/[L]$ and taking the y-intercept as representing 1 μM of bound ligand, i.e. under ligand-saturating conditions when the enzyme active sites would be expected to be fully occupied with ligand. Sodium cholate (0.15 % w/v) and glycerol (20 % v/v) were included to prevent the substrates from precipitating out of solution and to help stabilize the proteins.

The conversion of P450 Fe^{II}–CO into P420 Fe^{II}–CO

The CYP17 mutant, Glu^{305} → Gln : Thr^{308} → Ala (7 μM, 300 μl), in a potassium phosphate buffer [50 mM, pH 7.25, glycerol (20 % v/v) and sodium cholate (0.15 % w/v)] and buffer only, were placed in the sample and reference cuvettes respectively and a baseline recorded. A few crystals of sodium dithionite were added to the sample cuvette, carbon monoxide was bubbled through for 90 s and an absorption spectrum was recorded. After incubating at 30 °C for 80 min a final absorption spectrum was

taken (Figure 2A). The stability of the ferrous–carbon monoxide complex of the various CYP17 proteins was then measured by monitoring the shift of the Soret absorption peak from 447 to 422 nm. A 1 ml solution of the purified CYP17 protein [1 μM, in potassium phosphate buffer, 50 mM, pH 7.25, glycerol (20 % v/v) and sodium cholate (0.15 %w/v)] was reduced by the addition of sodium dithionite crystals, separated into sample and reference cuvettes and carbon monoxide bubbled through the sample cuvette for 90 s. Absorbances at wavelengths 500, 447 and 422 nm were recorded at 30 s intervals over a period of 1 h. The decrease and increase in absorbance at wavelengths 447 and 422 nm, respectively, were plotted against time; the intercept of the curves equated to the $t_{\frac{1}{2}}$ of the P450 Fe^{II}–CO complex – this was confirmed by fitting the 447 nm curve to monoexponential (first-order) decay analysis.

RESULTS

Enzymological studies

In Table 2 are presented the three activities of the wild-type enzyme, showing that the hydroxylase reaction, converting pregnenolone (**1**) into 17α-hydroxypregnenolone (**2**) was moderately stimulated by cytochrome b_5 while the side-chain cleavage of **2** into the androgen DHEA (**3**), using the lyase activity, was stimulated almost 10-fold in the presence of cytochrome b_5. This high degree of dependence of the lyase reaction on cytochrome b_5 is unique for the human isoform of CYP17 and has been ascribed a regulatory function in previous reports [26,27]. The results in Table 2 further show that the carbaldehyde (**4**), a specially designed analogue [11], is handled by CYP17 3- to 4-fold better than any of the physiological substrates. Two features of the reaction with the carbaldehyde (**4**) meriting comment are that the acyl-carbon cleavage with this analogue produces two products (**5** + **6**) and the process is not significantly stimulated by cytochrome b_5 [11]. For the sake of economy, therefore, in this study all the kinetic experiments with the carbaldehyde (**4**) were performed only in the absence of cytochrome b_5, after having confirmed that cytochrome b_5 also had a negligible effect with the $Glu^{305} \rightarrow Gln$ and $Glu^{305} \rightarrow Gln : Thr^{308} \rightarrow Ala$ mutants (data not shown).

It should be mentioned that the use of three different reactions to monitor the activities of the various mutant enzymes provided critical information on important issues. For example, the fact that the cleavage of the carbaldehyde (**4**) by the mutants, with one exception, occurred at rates which were greater than the rate of maximum hydroxylation displayed by the wild-type enzyme ensured that the impairment of the hydroxylation reaction, when observed, was not the consequence of gross protein conformational changes. Furthermore, in the comparison of the three activities, the effects, if any, of mutations on the rate of electron transport or the reduction of oxygen will be cancelled since these processes are common to all the three reactions.

The $Glu^{305} \rightarrow Gln$ mutant catalysed all the three reactions at respectable rates that were between 21 and 49 % of those with the wild-type enzyme, in particular the hydroxylation reaction (**1** → **2**, Scheme 1) occurred at 35 % of the rate shown by the wild-type enzyme (Table 2). Of the single mutations, the replacement of Thr^{306} with Ala had the greatest effect; whereas the rate of the hydroxylation reaction was reduced to 6 %, the impairment of the two acyl-carbon cleavage reactions was less extensive and these reactions occurred at 29–42 % of the wild-type rate. This facet is further emphasized when the activities of the various constructs to promote the cleavage of the carbaldehyde (**4**) – the more favourable of the two acyl-carbon cleavages studied in this work – are compared with those for the hydroxylation reactions in the presence of cytochrome b_5. The ratio of the two activities (aldehyde cleavage : hydroxylation; Table 2) for the wild-type enzyme was found to be 3.5 that increased to 25.6 for the $Thr^{306} \rightarrow Ala$ single mutant and more than 48.5 for the $Glu^{305} \rightarrow Ala : Thr^{306} \rightarrow Ala$ double mutant. This differential effect of the Thr^{306} mutation on the two activities is reminiscent of the findings on the $Thr^{302} \rightarrow Ala$ mutant of *P*-450 2B4 that, compared to the wild-type enzyme, showed greatly increased acyl-carbon cleavage over hydroxylase activity [10].

In the primary sequence of CYP17, the active site Thr^{306} is adjacent to a cluster comprising two Thr and a Ser residue (see top row, Table 1). These residues were also mutated and in general, the effect of their mutation on enzyme activity decreased as the position modified moved away from the Thr^{306} (and thus the putative active site region); the order of impairment of activity was: $Thr^{306} \rightarrow Ala > Thr^{307} \rightarrow Ala > Ser^{309} \rightarrow Ala > Thr^{308} \rightarrow Ala$. In fact, the $Thr^{308} \rightarrow Ala$ mutant was marginally more active than its wild-type counterpart. Three double mutants were also examined in which the active site Glu^{305} and another hydroxy amino acid residue were altered. The double mutant $Glu^{305} \rightarrow Gln : Thr^{306} \rightarrow Ala$, as expected, produced an enzyme with negligible hydroxylase and lyase activities, but significantly showed about 8 % of the wild-type activity in the acyl-carbon cleavage of the carbaldehyde (**4**). The other two double mutants involved the same Glu^{305} but now with Thr^{308} and Ser^{309}, shown to be non-essential residues by their single mutation experiments in Table 2. The $Glu^{305} \rightarrow Gln : Ser^{309} \rightarrow Ala$ double mutant catalysed the two physiological reactions (**1** → **2** and **2** → **3**) at 26 and 16 % of the wild-type rate respectively but showed a high activity for the cleavage of the carbaldehyde. The $Glu^{305} \rightarrow Gln : Thr^{308} \rightarrow Ala$ mutant displayed a similar profile and had 45, 20 and 88 % of the wild-type activity for the hydroxylase, lyase and carbaldehyde cleavage respectively. Thus the enzymic properties of the various mutant enzymes show that the two active site residues, Glu^{305} and Thr^{306}, are not directly involved in a catalytic role.

Using the two physiological substrates (**1** and **2**), the spectral dissociation constants of the various CYP17 proteins were determined. The data in Tables 2 and 3 show that, overall, the mutants that were poor catalysts also had lower affinities for the two substrates and that, as might be expected, the double mutants had lower substrate affinities than their single mutant counterparts. Interestingly the single mutation involving the active site Glu^{305} made greater contributions to the increase in K_s value than did those of the four hydroxy amino acid residues.

Table 3 Substrate dissociation constants and the $t_{\frac{1}{2}}$ values for the rearrangement of the 450 nm → 420 nm species

Experiments were performed in triplicate with the data expressed as means ± S.E.

CYP17 variant	K_s (μM, at 12 °C) Pregnenolone	K_s (μM, at 12 °C) 17-OH preg	$t_{\frac{1}{2}}$ (min, at 30 °C) *P*-450 Fe^{II}–CO
Wild-type	0.75 ± 0.10	1.16 ± 0.08	13.7 ± 0.7
Glu^{305} → Gln	1.85 ± 0.20	7.10 ± 0.40	9.0 ± 0.5
Thr^{306} → Ala	1.43 ± 0.10	2.87 ± 0.13	9.6 ± 0.4
Thr^{307} → Ala	1.58 ± 0.12	2.80 ± 0.20	11.4 ± 0.6
Thr^{308} → Ala	0.92 ± 0.08	1.80 ± 0.12	14.7 ± 0.8
Ser^{309} → Ala	1.15 ± 0.10	2.87 ± 0.08	11.8 ± 0.8
Glu^{305} → Ala : **Thr^{306}** → Ala	4.10 ± 0.30	7.60 ± 0.20	5.9 ± 0.6
Glu^{305} → Ala : Thr^{308} → Ala	3.55 ± 0.15	10.07 ± 1.0	14.8 ± 1.0
Glu^{305} → Ala : Ser^{309} → Ala	2.97 ± 0.17	9.80 ± 0.20	8.3 ± 0.4

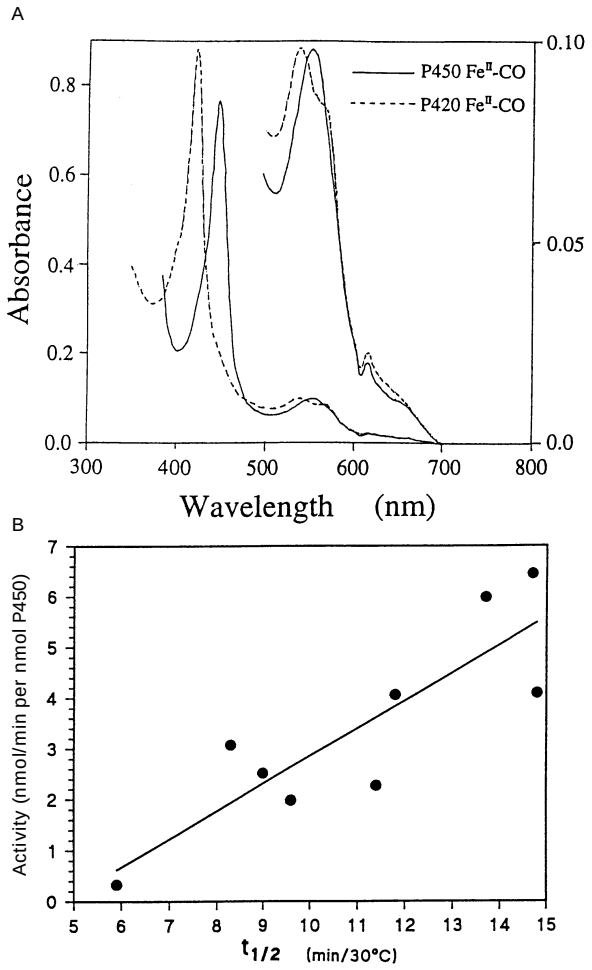

Figure 2

(**A**) *P*-450 and *P*-420 ferrous–carbon monoxide binding absorption spectra for the CYP17 mutant, $Glu^{305} \rightarrow Gln:Thr^{308} \rightarrow Ala$. The 420 nm species has all the major identifiable spectral characteristics of the P420 ferrous–carbon monoxide binding absorption spectra [28]: its Soret peak at 422 nm and maxima at 540 and 572 nm (the latter is seen here as a shoulder). (**B**) The correlation between activity and stability for the various mutant CYP17 proteins. For each CYP17 protein its three activities (Table 2) were summed and the mean value plotted against the $t_{\frac{1}{2}}$ values for the conversion of the 450 nm into the 420 nm species.

$t_{\frac{1}{2}}$ of the conversion of *P*-450 into *P*-420

P-450s have the tendency to undergo a subtle but stable conformational rearrangement in the haem-binding region of the protein that causes the Soret absorption peak of the Fe^{II}–CO complex to shift from 450 to 420 nm [28] (Figure 2A). We exploited the 450 → 420 nm conversion as a probe of the stability of the active site architecture of the various mutant CYP17 proteins, by measuring the $t_{\frac{1}{2}}$ values of the rearrangement. Table 3 shows that the wild-type protein has one of the most stable structural makeups and gave a $t_{\frac{1}{2}}$ for the conversion of *P*-450 → *P*-420 of 13.7 min at 30 °C while the catalytically least active double mutant ($Glu^{305} \rightarrow Gln:Thr^{306} \rightarrow Ala$, Table 2) had the shortest value of 5.9 min. In broad terms there seems to be a correlation between the activity of a protein and its propensity to undergo the rearrangement, the more active the protein the less readily did it rearrange (see Figure 2B). It should be noted that the rearrangement does not affect the data in Table 2 since the activities for all the CYP17 proteins were linear throughout their measured time course and that the most unstable of these mutants ($Glu^{305} \rightarrow Gln:Thr^{306} \rightarrow Ala$) displayed less than 25% conversion of *P*-450 to *P*-420 under the assay conditions, in which the enzyme is present in lipid vesicles (data not shown).

DISCUSSION

Scheme 2 summarizes our original proposal showing that the hydroxylation and acyl-carbon cleavage reactions catalysed by multicatalytic P450s, for example, CYP17, occur using two distinct forms of oxygenated intermediates. The hydroxylation reaction uses the conventional iron-monooxygen species (**10**) while the acyl-carbon cleavage uses an iron-peroxy intermediate (**8**). The involvement of **8** in the cleavage was originally suggested from the results of isotopic experiments on aromatase (CYP19), showing the incorporation of an atom of oxygen from $^{18}O_2$ into C-19, released as formate [1,7,29] [cf eqn. (1)]. It was subsequently found that in some cases the carbon radical (**15**) arising from the acyl-carbon cleavage not only underwent disproportionation to the corresponding double bond (**15** → **16**) but also followed alternative courses, characteristic of radical recombinations [9,30], particularly oxygen-rebound to produce a hydroxy compound (**15** → **17**) [11,31]. The fact that for CYP17 the formation of such an hydroxy compound (**6**) exclusively occurred at the expense of an acyl-carbon cleavage, without disturbing any other neighbouring bond, and that the process was shown to be formally a dioxygenase reaction, made it mandatory that a dioxygen species, e.g. Fe^{III}–O–O^- is involved in the transformation [11,31].

The requirement for acid catalysis in certain reactions, shown in Scheme 2, is similar to that considered by other workers for related processes [10,32]. In the Scheme the iron-peroxide anion (**8**), formed from the resting state of the *P*-450 using two single electrons plus O_2 [3,33–37], undergoes protonation at two successive stages (**8** → **9** and **9** → **10**) [37], to produce the oxo-derivative (**10**). There was a general consensus for some time that the oxo-derivative participates in the hydroxylation process by a stepwise radical mechanism (**10** → **11** → **12**) [34,35,38–40]. However, recently two other mechanistic variants have been considered, either involving **10** in a nonsynchronous concerted process [41] or using the Fe^{III}–OOH species as the ultimate hydroxylating agent [42]. The requirement for acid catalysis, though, is the same for all these alternatives.

Inherent in the proposal of Scheme 2 is the assumption that the juxtapositioning of the nucleophilic peroxide anion (**8**) and the electrophilic carbonyl group of the substrate is the main driving force for the formation of the adduct **13**, which directs the enzymic flux toward the acyl-carbon cleavage. The non-protonated form of the oxyanion in **13** is envisaged to undergo homolytic cleavage of the O–O bond to generate **14**, the latter then fragments to release the acetate ion.

According to the line of reasoning above the most economical route for the acyl-carbon cleavage is one where protonation is required only for the regeneration of the enzyme (Fe^{III}–OH + H^+ → **7**, Scheme 2), after all the bonding changes in the substrate skeleton have been completed. The latter scenario contrasts with the chemistry underpinning the hydroxylation process where the double protonation is a compulsory prerequisite for producing the catalytically component intermediate (**10**) capable of promoting the bonding changes in the substrate [37].

What then is the source of these protons? In cytochrome $P\text{-}450_{cam}$ Asp^{251} and Thr^{252} are located in the active site region of the enzyme and have been implicated in proton donation to the iron-peroxy species (**8**) during oxygen activation [43,44]. These two residues are conserved in many *P*-450s and correspond to

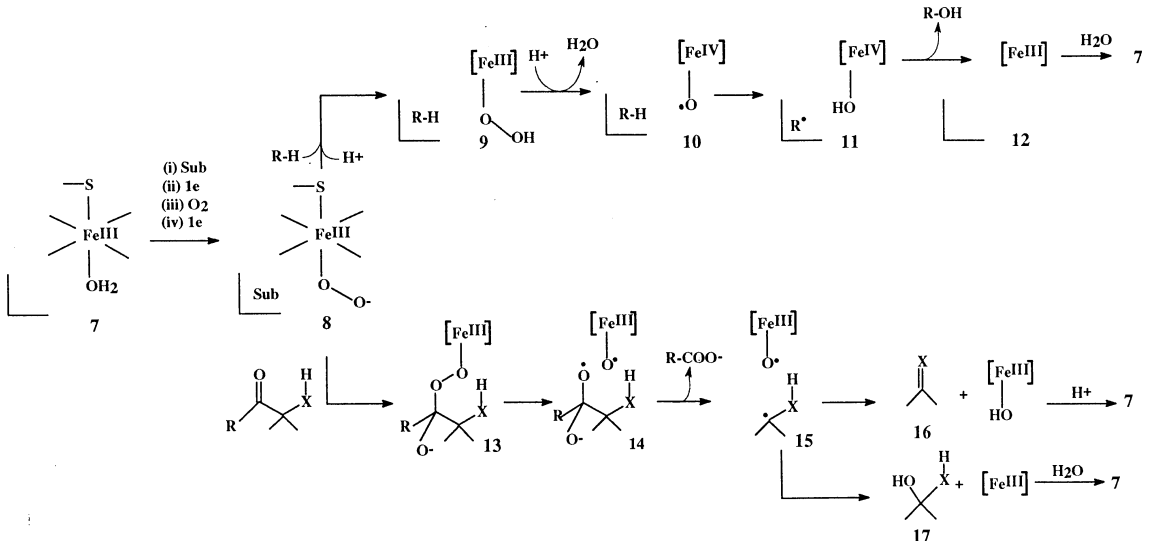

Scheme 2 The iron-peroxide intermediate is directed towards the hydroxylation or acyl-carbon bond cleavage pathway depending on the nature of the functional group in the substrate

The two proton-requiring steps are **8** → **9** and **9** → **10**. The oxo-derivative (**10**) has a number of canonical forms [e.g. $Fe^{V}=O \leftrightarrow (\dot{+})Fe^{IV}=O \leftrightarrow Fe^{IV}-O^{\bullet}$] and the one selected here shows the mechanism of the hydroxylation reaction most simply. The reactions involved in the acyl-carbon cleavage are: nucleophilic addition (**8** → **13**); homolytic cleavage (**13** → **14**); fragmentation (**14** → **15**); disproportionation (**15** → **16**) and oxygen-rebound (**15** → **17**). X = carbon or oxygen.

Glu^{305} and Thr^{306} in the sequence of CYP17. Therefore, the focus of the present study was 2-fold; to examine the role of Glu^{305} and Thr^{306}, and also to scrutinize the suggestion of Scheme 2. To achieve this single and double mutations were introduced at these two active site protic residues, Glu^{305} and Thr^{306}, and at three other adjacent residues (Thr^{307}, Thr^{308} and Ser^{309}). The cumulative results in Table 2 clearly show that none of the three adjacent residues, nor the active site Glu^{305}, is essential for catalysis. The acidic residue equivalent to Glu^{305} of CYP17 has been mutated in several microsomal *P*-450s when the mutant protein were found to have reduced hydroxylation activities [45,46] but in most cases the impairment of the activity was not so large to justify the direct involvement of the active site acidic residue in catalysis; by direct we mean the manner, for example, in which the acidic group in lysozyme takes part in the scission of the glycosidic bond.

In considering the role of the active site hydroxy amino acid residue, Thr^{306}, we found that its mutation to a neutral residue, $Thr^{306} \rightarrow Ala$, caused a greater reduction in hydroxylation than in acyl-carbon cleavage activity (right-hand column, Table 2). The differential effect on the two activities provides further support for the proposal of Scheme 2, in which these processes are shown to occur using different chemistries which also happen to differ in the requirement for acid catalysis.

Apart from the possibility of differing requirements for protonation in the critical stages of the two processes, the hydroxylation and acyl-carbon cleavage reactions differ in certain other respects. The reactive species, $Fe^{III}-O-O^{-}$, involved in the cleavage reaction not only possesses free rotation around the iron–oxygen bond but has a longer iron–dioxygen arm to reach the carbonyl group of the substrate for a nucleophilic attack. These features of the nucleophile together with the possibility of rotation around the carbonyl–carbon bond of the substrate allow adjustment in the position of the reacting groups to produce **13**. The formation of this key intermediate (**13**) may hence be relatively insensitive to minor changes in the geometry of the active site. On the other hand for the hydroxylation reaction to occur the $(\dot{+})Fe^{IV}=O$ bond of haem and the H–C bond of the substrate need to be very precisely aligned. This is to be achieved within the constraint that the reactive oxygen, of $(\dot{+})Fe^{IV}=O$, is close to the porphyrin iron atom, and though the H–C bond of the substrate is free to rotate, this rotation cannot alter its position with respect to the $(\dot{+})Fe^{IV}=O$ bond, unless the entire substrate skeleton were to move. The geometrical constraints on the hydroxylation reaction are thus more stringent than those for the acyl-carbon cleavage. This feature is more readily recognizable with the acyl-carbon cleavage of the analogue carbaldehyde (**4**) than with that of the physiological substrate (**2**). In the cleavage of (**4**), not only is its carbonyl more electrophilic compared with the ketone group of **2** for trapping the peroxide nucleophile, but also the site of reaction C-20 has a greater degree of freedom of rotation because of the absence of the C-21 methyl group, which in the physiological substrate seems to contribute to additional interactions with the enzyme [47].

Regarding the source of the protons, the cumulative results presented here and also by other workers may be interpreted to suggest that the proton delivery is directly performed neither by the OH group of the active site threonine [48–50] nor the carboxylate group of the adjacent acidic amino acid residue [51], yet both these residues are, to varying extents, important in the hydroxylation reaction promoted by *P*-450s. In search of the eventual source of the protons used in the O–O bond cleavage we further develop the thesis originally considered by Kimata et al. [52] to explain the results of the $Thr^{252} \rightarrow MeO-Thr$ mutant of $P\text{-}450_{cam}$, subsequently supported by the X-ray structure of $P\text{-}450_{eryF}$ [53], which lacks the active-site hydroxy-amino-acid residue, and also by other mutational studies [48–51]. According to these, water may be the eventual source of the protons used in steps **8** → **9** and **9** → **10** of the hydroxylation process (Scheme 2). It is possible that the H_2O molecules involved in proton delivery are strategically harnessed, with respect to the orientation of the

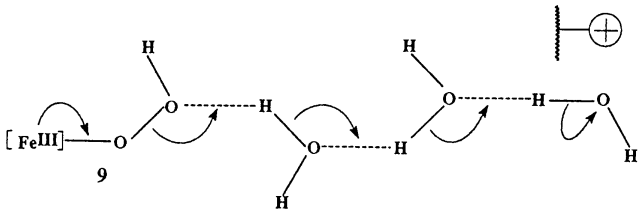

Scheme 3 Showing the dissipation of the hydroxide ion released following proton delivery

The conversion of the Fe^{III}–OOH (**9**) into the oxo derivative (**10**). The terminal H_2O molecule in the charge relay system faces either the bulk solvent or a strategically located cationic residue (i.e. the side chain of either a lysine or arginine).

O–O bond of two intermediates (**8** and **9**), by polydentate interactions in which two active site amino acids, somehow, play important but not exclusive roles, hence the mutation of either is only partially debilitating. Thus depending on the chemical nature of and specific contribution made by other supporting functional groups, the effects of the mutations of the two active site residues vary from one *P*-450 to another and give rise to subtle changes in the active site region of the protein. In this connection the data on the $t_{\frac{1}{2}}$ of the rearrangement of the 450 nm to the 420 nm species are particularly instructive. These results highlight that the extent of perturbation of the protein structure, caused by a mutation, from its ideal geometry in the wild-type protein, is correlated to the impairment of its catalytic activity; thus the $t_{\frac{1}{2}}$ values for the rearrangement of the most and the least active catalysts were on two extremes (Figure 2B).

The water molecule involved in proton delivery may be regarded as yet another substrate for *P*-450s. The first molecule of water participating in proton donation might be the one released from the coordination shell of the iron upon substrate binding. The ability of a H_2O molecule, held at the active site of an enzyme by a network of hydrogen bonds, to act as proton donor in reaction (**8** → **9**) is not difficult to envisage from a chemical view point; since the p*K* values of the peroxide (about 13.0) and water (about 15) are within 2 units, which would permit proton transfer at a diffusion control rate [54]. On the other hand the cleavage of the O–O bond of a peroxide will normally be expected to have a more demanding requirement for acid catalysis. In the reaction **9** → **10** (Scheme 2), however, the cleavage process could be partly driven by the intrinsic chemistry of the iron-peroxide bond, in which electron release from the metal provides the primary driving force. Notwithstanding these considerations, for H_2O to act effectively in the role assigned above, it may be desirable that the two proton delivery steps are temporally coupled to the arrival of a cationic species for the neutralization of the released hydroxide ions. Alternatively another mechanism may be available which allows a facile exit of HO^- from the interior of the protein into the bulk solvent as illustrated in Scheme 3. A water channel has been identified in the Fe^{III} form of $P\text{-}450_{cam}$ [55] but the water molecules in the channel do not seem to be close enough to the haem iron to be the candidate for the acid catalyst required in Scheme 2. However, recent NMR studies on $P\text{-}450_{bm\text{-}3}$ have shown that the conversion of the Fe^{III} substrate into the Fe^{II} substrate complex is attended by a large conformational change in the region surrounding the haem prosthetic group [56]; such a change could bring these water molecules in close proximity to the active site for engaging them in catalysis.

We thank J. Neville Wright for providing the tritiated substrates and helpful discussions. This work was supported by the BBSRC.

REFERENCES

1 Akhtar, M., Corina, D. L., Pratt, J. and Smith, T. (1976) J Chem. Soc., Chem. Commun. 854–856
2 Stevenson, D. E., Wright, J. N. and Akhtar, M. (1985) J. Chem. Soc., Chem. Commun. 1078–1080
3 Akhtar, M. and Wright, J. N. (1991) Natl. Prod. Rep. **8**, 527–551
4 Wright, J. N. and Akhtar, M. (1990) Steroids **55**, 142–151
5 Akhtar, M., Njar, V. C. and Wright, J. N. (1993) J. Steroid Biochem. Mol. Biol. **44**, 375–387
6 Akhtar, M., Lee-Robichaud, P., Akhtar, M. E. and Wright, J. N. (1997) J. Steroid Biochem. Mol. Biol. **61**, 127–132
7 Akhtar, M., Calder, M. R., Corina, D. L. and Wright, J. N. (1982) Biochem. J. **201**, 569–580
8 Roberts, E. S., Vaz, A. D. N. and Coon, M. J. (1991) Proc. Natl. Acad. Sci. U.S.A. **88**, 8963–8966
9 Raner, G. M., Chiang, E. W., Vaz, A. D. N. and Coon, M. J. (1997) Biochemistry **36**, 4895–4902
10 Vaz, A. D. N., Pernecky, S. J., Raner, G. M. and Coon, M. J. (1996) Proc. Natl. Acad. Sci. U.S.A. **93**, 4644–4648
11 Lee-Robichaud, P., Shyadehi, A. Z., Wright, J. N., Akhtar, M. and Akhtar, M. (1995) Biochemistry **34**, 14104–14113
12 Akhtar, M., Alexander, K., Boar, R. B., McGhie, J. F. and Barton, D. H. R. (1978) Biochem. J. **169**, 449–463
13 Shyadehi, A. Z., Lamb, D. C., Kelly, S. L., Kelly, D. E., Schunk, W.-H., Wright, J. N., Corina, D. and Akhtar, M. (1996) J. Biol. Chem. **271**, 12445–12450
14 Mansuy, D., Boucher, J. L. and Clement, B. (1995) Biochimie **77**, 661–667
15 Cole, P. A. and Robinson, C. H. (1988) J. Am. Chem. Soc. **110**, 1284–1285
16 Poulos, T. L., Finzel, B. C. and Howard, A. J. (1987) J. Mol. Biol. **195**, 687–700
17 Hasemann, C. A., Kurumbail, R. G., Boddupalli, S. S., Peterson, J. A. and Deisenhofer, J. (1995) Structure **3**, 41–62
18 Lewis, D. F. V. (1995) Xenobiotica **25**, 333–366
19 Nakajin, S. and Hall, P. F. (1981) J. Biol. Chem. **256**, 3871–3876
20 Akhtar, M., Corina, D. L., Miller, S. L., Shyadehi, A. Z. and Wright, J. N. (1994) J. Chem. Soc., Perkin Trans. 1 263–267
21 Kremers, P., Denoel, J. and Lapieve, C. J. (1974) Steroids **23**, 603–613
22 Imai, T., Globerman, H., Gertner, J. M., Kagawa, N. and Waterman, M. R. (1993) J. Biol. Chem. **268**, 19681–19689
23 Higuchi, R. (1990) in PCR Protocols. A Guide to Methods and Applications (Innis, M. A., Gelfand, D. H., Sninsky, J. J. and White, T. J., eds.), pp. 177–183, Academic Press Inc., London
24 Strobel, H. W. and Dignam, J. D. (1978) Methods Enzymol. **52**, 89–96
25 Strittmatt, P., Fleming, P., Connors, M. and Corcoran, D. (1978) Methods Enzymol. **52**, 97–101
26 Lee-Robichaud, P., Wright, J. N., Akhtar, M. and Akhtar, M. (1995) Biochem. J. **308**, 901–908
27 Katagiri, M., Kagawa, N. and Waterman, M. R. (1995) Arch. Biochem. Biophys. **317**, 343–347
28 Martinis, S. A., Blanke, S. R., Hager, L. P., Sligar, S. G., Hui Bon Hoa, G., Rux, J. J. and Dawson, J. H. (1996) Biochemistry **35**, 14530–14536
29 Stevenson, D. E., Wright, J. N. and Akhtar, M. (1988) J. Chem. Soc., Perkin Trans. 1 2043–2052
30 Coon, M. J., Vaz, A. D. N. and Bestervelt, L. L. (1996) FASEB J. **10**, 428–434
31 Akhtar, M., Corina, D., Miller, S., Shyadehi, A. Z. and Wright, J. N. (1994) Biochemistry **33**, 4410–4418
32 Swinney, D. C. and Mak, A. Y. (1994) Biochemistry **33**, 2185–2190
33 Gunsalus, I. C. and Sligar, S. G. (1978) Adv. Enzymol. **47**, 1–44
34 Groves, J. T. and Han, Y. (1995) in Cytochrome P-450: Structure, Mechanism and Biochemistry (Ortiz de Montellano, P. R., ed.), pp. 3–48, Plenum Press, New York
35 Ortiz de Montellano, P. R. (1995) in Cytochrome P-450: Structure, Mechanism and Biochemistry (Ortiz de Montellano, P. R., ed.), pp. 245–303, Plenum Press, New York
36 Coon, M. J., Ding, X., Pernecky, S. J. and Vaz, A. D. N. (1992) FASEB **6**, 669–673
37 Benson, D. E., Suslick, K. S. and Sligar, S. G. (1997) Biochemistry **36**, 5104–5107
38 Atkinson, J. K., Hollenberg, P. F., Ingold, K. U., Johnson, C. C., Le Tadic, M., Newcomb, M. and Putt, D. A. (1994) Biochemistry **33**, 10630–10637
39 Groves, J. T., McClusky, G., White, R. E. and Coon, M. J. (1978) Biochem. Biophys. Res. Commun. **81**, 154–160
40 Gelb, M. H., Heimbrook, D. C., Malkonen, P. and Sligar, S. G. (1982) Biochemistry **21**, 370–377
41 Newcomb, M., Le Tadic-Biadatti, M.-H., Chestney, D. L., Roberts, E. S. and Hollenberg, P. F. (1995) J. Am. Chem. Soc. **117**, 12085–12091

42 Pratt, J. M., Ridd, T. I. and King, L. J. (1995) J. Chem. Soc., Chem. Commun. 2297–2298
43 Imai, M., Shimada, H., Watanabe, Y., Matsushima-Hibiya, Y., Makino, R., Koga, H., Horiuchi, T. and Ishimura, Y. (1989) Proc. Natl. Acad. Sci. U.S.A. **86**, 7823–7827
44 Gerber, N. C. and Sligar, S. G. (1994) J. Biol. Chem. **269**, 4260–4266
45 Ellis, S. W., Hayhurst, G. P., Smith, G., Lightfoot, T., Wong, M. M. S., Simula, A. P., Ackland, M. J., Sternberg, M. J. E., Lennard, M. S., Tucker, G. T. and Wolf, C. R. (1995) J. Biol. Chem. **270**, 29055–29058
46 Hiroya, K., Murakami, Y., Shimizu, T., Hanato, M. and Ortiz de Montellano, P. R. (1994) Arch. Biochem. Biophys. **310**, 397–401
47 Depledge, N. W. (1997) Thesis, University of Southampton, U.K.
48 Yeom, H., Sligar, S. G., Li, H., Poulos, T. L. and Fulco, A. (1995) Biochemistry **34**, 14733–14740
49 Fukada, T., Imai, Y., Komori, M., Nakamura, M., Kusunose, E., Satouchi, K. and Kusunose, M. (1993) J. Biochem. (Tokyo) **113**, 7–12
50 Ishigooka, M., Shimizu, T., Hiroya, K. and Hatano, M. (1992) Biochemistry **31**, 1528–1531
51 Yeom, H. and Sligar, S. G. (1997) Arch. Biochem. Biophys. **337**, 209–216
52 Kimata, Y., Shimada, H., Hirose, T. and Ishimura, Y. (1995) Biochem. Biophys. Res. Commun. **208**, 96–102
53 Cupp-Vickery, J. R. and Poulos, T. L. (1995) Nature Struct. Biol. **2**, 144–153
54 Eigen, M. (1964) Angew. Chem. Int. Ed. Engl. **3**, 1–72
55 Oprea, T. I., Hummer, G. and Garcia, A. E. (1997) Proc. Natl. Acad. Sci. U.S.A. **94**, 2133–2138
56 Modi, S., Sutcliffe, M. J., Primrose, W. U., Lian, L. and Roberts, G. C. K. (1996) Nature Struct. Biol. **3**, 414–417

Received 2 September 1997/10 November 1997; accepted 1 December 1997